Polar boundary layer bromine explosion and ozone depletion events in the chemistry-climate model EMAC v2.52: Implementation and evaluation of AirSnow algorithm

Stefanie Falk[1] and Björn-Martin Sinnhuber[1]

[1]Institute of Meteorology and Climate Research, Karlsruhe Institute of Technology, Karlsruhe, Germany

Correspondence to: Björn-Martin Sinnhuber (bjoern-martin.sinnhuber@kit.edu)

Abstract. Ozone depletion events (ODE) in the polar boundary layer have been observed frequently during spring-time. Most likely, they are related to events of boundary layer enhancement of bromine. Consequently, increased vertical column densities (VCD) of BrO have been observed from satellites. These so called bromine explosion events have been discussed serving as source of tropospheric BrO at high latitudes. We have implemented a treatment of bromine release and recycling on sea ice and snow covered surfaces in the global chemistry-climate model EMAC (ECHAM/MESSy Atmospheric Chemistry) based on the scheme of Toyota et al. (2011). In this scheme, dry deposition fluxes of HBr, $HOBr$, and $BrNO_3$ over ice and snow covered surfaces are recycled into Br_2 fluxes. In addition, dry deposition of O_3, dependent on temperature and sunlight, triggers a Br_2 release from surfaces associated with first-year sea ice. Many aspects of observed bromine enhancements and associated episodes of near-complete depletion of boundary layer ozone, both in the Arctic and in the Antarctic, are reproduced by this relatively simple approach. We present first results from our global model studies extending over a full annual cycle, including comparisons with GOME satellite BrO VCD and surface ozone observations.

1 Introduction

Events of near-complete depletion of polar boundary layer ozone are observed frequently during spring-time over both hemispheres (Oltmans, 1981; Bottenheim et al., 1986, 2002, 2009). Individual events typically last between several hours to a few days. The boundary layer ozone depletion events (ODE) are almost certainly related to events of strongly enhanced bromine, so called bromine explosion events. Enhanced bromine monoxide (BrO) column densities are regularly observed from satellites over both hemispheres, predominantly over the marginal sea ice zone, but sometimes also over inland ice and snow covered regions (e.g., Richter et al., 1998). In addition to their impact on boundary layer ozone, bromine explosion events play an important role in mercury deposition and corresponding environmental impacts (Lindberg et al., 2002; Stephens et al., 2012). Proposed mechanisms for bromine explosion events involve frost flowers on thin sea ice (Kaleschke et al., 2004) and blowing of saline snow on sea ice (Yang et al., 2010). Carbonate precipitation in brine at low temperatures has been suggested as efficient release trigger of sea-salt bromine to the atmosphere (Sander et al., 2006). However, measurements of Br_2 release in dependence of illumination and ozone volume mixing ratio (VMR) from various types of snow and ice indicate that neither sea ice itself nor brine icicles are a source for Br_2 but snow on land surfaces has to be taken into consideration (Pratt et al.,

2013). Recent reviews are provided by Simpson et al. (2007), Saiz-Lopez and von Glasow (2012), and Custard et al. (2015). In spite of progress in describing the mechanisms involved in bromine release and boundary layer ODE, existing modeling approaches still rely on a number of semi-empirical assumptions. Toyota et al. (2011) presented a parametrization within the Global Environmental Multiscale model with Air Quality processes (GEM-AQ). GEM-AQ is based on Canada's operational weather prediction model developed by the Meteorological Services of Canada (MSC) for the interaction of atmospheric chemistry with sea ice and snow surfaces. This parametrization reproduces many aspects of observed bromine enhancements and boundary layer ODE.

Here we present an implementation of a mechanism based on the work of Toyota et al. (2011) into the ECHAM/MESSy Atmospheric Chemistry (EMAC) model (Jöckel et al., 2010). The mechanism and its integration into the existing submodel ONEMIS (Kerkweg et al., 2006) are described in Sect. 2. In Sect. 3, results from one year long integrations of the model with and without bromine release are presented and compared to surface ozone observations as well as observations of tropospheric BrO vertical column density (VCD) from the Global Ozone Monitoring Experiment (GOME) satellite instrument on board ERS-2 (Richter et al., 1998, 2002). We show that many aspects of observations regarding BrO enhancements and ODE are reproduced by this mechanism without any further tuning of parameters. Unlike most previous modeling studies, we do not focus on Arctic spring time only but investigate a full annual cycle on both hemispheres.

2 Model and experiments

The EMAC model is a numerical chemistry-climate model, based on 5th generation European Centre Hamburg general circulation model (ECHAM5) (Roeckner et al., 2006) as dynamical core. Various submodels describe atmospheric and Earth system processes and are coupled via the Modular Earth Submodel System (MESSy). MESSy provides an infrastructure with generalized interfaces for control and coupling of components. Further information about MESSy and EMAC is available from the MESSy project homepage. MESSy enables for a flexible handling of emissions in EMAC, e.g., prescribed fluxes, (boundary) layer concentrations of tracers, and emissions dependent on dynamical atmospheric fields. Latter are treated as *online* emissions using the submodel ONEMIS (Kerkweg et al., 2006). ONEMIS provides facility functions for flux to tracer concentration conversions. According to the MESSy philosophy, ONEMIS is separated into a submodel interface layer (smil) for unified data handling among different submodels and an implementation layer of the actual emission mechanisms (smcl). A recap of the mechanism proposed by Toyota et al. (2011) (Sect. 2.1) and details about its integration into the EMAC model (Sect. 2.2) are given in the following. In Sect. 2.3, scope and setup of the test experiments are summarized.

2.1 Description of the mechanism

It is assumed that at least part of the observed Br_2 flux originates from heterogeneous reactions on snow grains in the surface layer of a snowpack (Pratt et al., 2013). These snow grains are considered coated by a Br^- enriched film of liquid water and show a distinct acidity. In this quasi-liquid phase, heterogeneous reactions of HOBr and $BrNO_3$ with either Br^- and Cl^- can

take place:

$$HOBr + Br^- \xrightarrow{H^+} Br_2 + H_2O, \tag{R1}$$

$$BrNO_3 + Br^- \rightarrow Br_2 + NO_3^-, \tag{R2}$$

$$HOBr + Cl^- \xrightarrow{H^+} BrCl + H_2O, \tag{R3}$$

$$BrNO_3 + Cl^- \rightarrow BrCl + NO_3^-. \tag{R4}$$

Interhalogene reactions may convert $BrCl$ into Br_2:

10    $$BrCl + Br^- \leftrightarrow Br_2Cl^- \leftrightarrow Br_2 + Cl^- \tag{R5}$$

$BrCl$ is partly released to the atmosphere before undergoing this last reaction. Another reaction pathway is actually triggered by ozone dry deposition under the influence of sunlight. This pathway accumulates various gas, aqueous, and heterogeneous phase reactions (for details see Pratt et al., 2013, Fig. 2). Toyota et al. (2011) have parametrized these heterogeneous reaction pathways ($HOBr$ / $BrNO_3$ / $O_3 \rightarrow Br_2$) in a simple way.

15   Three surface types, first-year sea ice (FY), multi-year sea ice (MY), and snow on land (LS) are differentiated. In any case, the respective surface temperature has to be below a temperature threshold T_{crit}. The conversion of a dry deposition flux of ozone (Φ_{O_3}) into an emission flux of Br_2 (or $BrCl$) is moderated by an ad hoc molar yield Φ_1, dependent on surface type and illumination:

$$\Phi_1 = \begin{cases} 0.001 & \text{if } \textit{dark} \text{ FY}, \\ 0.075 & \text{if } \textit{sunlit} \text{ FY}, \\ 0 & \text{if MY and LS}. \end{cases} \tag{1}$$

20   I.e., on FY sea ice, only 0.1% of the dry deposition of O_3 will be converted into Br_2 if the sun's zenith angle is above $\theta_{crit} = 85\,^\circ$, otherwise 7.5% is converted. No release of Br_2 from MY sea ice or LS is assumed.

The conversion of dry deposition fluxes of $HOBr$ (Φ_{HOBr}), $BrNO_3$ (Φ_{BrNO_3}), and HBr (Φ_{HBr}) is considered independent of illumination. In case of FY sea ice, the snow pack on top is regarded as an infinite pool of Br^- and Cl^-. The sum of $HOBr$ and $BrNO_3$ dry deposition fluxes ($\Phi_{HOBr} + \Phi_{BrNO_3}$) is fully recycled into Br_2. In case of MY sea ice, only the Cl^- pool remains

25   infinite, for Cl^- is about 2 to 3 orders of magnitude more abundant in snow than Br^- (Toyota et al., 2011). The release of Br_2 depends on $\Phi_{HOBr} + \Phi_{BrNO_3}$ in comparison to the dry deposition flux of HBr. If $\Phi_{HOBr} + \Phi_{BrNO_3}$ was less than Φ_{HBr} a full
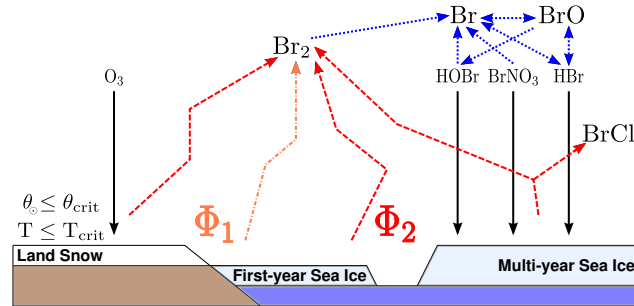
Figure 1. Schematic scenario of bromine release from first-year sea ice, multi-year sea ice, and land snow adapted from Toyota et al. (2011) for a temperature threshold T_{crit}. Black arrows denote dry deposition of HOBr, BrNO$_3$, HBr, and O$_3$. Blue doted arrows indicate gas-phase photochemistry. Dry deposition fluxes are recycled into Br$_2$ with respect to a molar yield Φ_1 in case of O$_3$ (dashed orange) and Φ_2 in case of the brominated species (dashed red).

conversion of $\Phi_{\mathrm{HOBr}} + \Phi_{\mathrm{BrNO_3}}$ to Br$_2$ is assumed. Otherwise, only half of the difference $\Phi_{\mathrm{HOBr}} + \Phi_{\mathrm{BrNO_3}} - \Phi_{\mathrm{HBr}}$ is recycled to Br$_2$, the other half is converted to BrCl. For LS, neither Br$^-$ nor Cl$^-$ is available unlimited. Hence, only the smaller of $\Phi_{\mathrm{HOBr}} + \Phi_{\mathrm{BrNO_3}}$ and Φ_{HBr} is converted to Br$_2$. The resulting *yield* is summarized in Φ_2:

$$\Phi_2 = \begin{cases} 1 & \text{if FY}, \\ 0.5 - 1 & \text{if MY}, \\ 0 - 1 & \text{if LS}. \end{cases} \tag{2}$$

5 Schematically, all release scenarios are shown in Fig. 1 (adapted from Fig. 1 of Toyota et al. (2011)). Herein, black arrows denote dry deposition of HOBr, BrNO$_3$, HBr, and O$_3$. Blue doted arrows indicate gas-phase photochemistry. The recycled fluxes are displayed by dashed orange (O$_3$) and red (HOBr, BrNO$_3$, HBr) arrows.

2.2 Implementation

10 In accordance to the described scheme, submodel interface, submodel core, and namelist of ONEMIS have been extended based on EMAC version 2.52. Channel objects, which are used by a subroutine `airsnow_emissions`, include surface temperature (`tsurf`), fraction of snow cover on land (`cvs`), fraction of ice cover on ocean (`seaice`), cosine of sun's zenith angle (`cossza`), and dry deposition fluxes of HOBr, BrNO$_3$, HBr, and O$_3$ (`drydepflux_<HOBr, BrNO3, HBr, O3>`). Dry deposition is computed by submodel DDEP (formerly DRYDEP, Kerkweg et al., 2006, b). Additional information about
15 multi-year sea ice cover (MYSIC) has to be provided through data import. Steering parameters, Φ_1, T_{crit}, and θ_{crit}, can be changed in the corresponding control sequence within the ONEMIS namelist file. However, the parameter relevant to MY sea ice and LS in Φ_1 is currently not used, since no parametrization has been provided by Toyota et al. (2011). New output channels `snow_air_flux_br2` and `snow_air_flux_brcl` have been defined. Instead of actual code, a Nassi-

Shneiderman diagram displaying the algorithm implemented in subroutine `airsnow_emissions` in more detail is provided in Supplement S.1. The new emission mechanism has been named *AirSnow* and can be switched on in the ONEMIS namelist – an example excerpt has been added as Supplement S.2.

2.3 Validation Experiments

5 Three experiments have been performed using EMAC version 2.52 (see Table 1 for a summary). The basic model setup has been adapted from RC1SD-base-08, which is part of a Chemistry-Climate Model Initiative (CCMI) recommended set of simulations by the Earth System Chemistry-Climate Modelling (ESCiMo) consortium (Jöckel et al., 2016). The model integrations use specified dynamics nudged to ERA-Interim for the year 2000. Accordingly, ERA-Interim sea ice cover (SIC) has been used. The chosen spatial resolution is T42L90MA corresponding to a $2.8° \times 2.8°$ grid, with a top level at $0.01\,\mathrm{hPa}$ and distributed to

10 90 levels. Output has been saved with one hourly temporal resolution. In contrast to RC1SD-base-08, fluxes of brominated very short-lived substances (VSLS), CH_2Br_2 and $CHBr_3$, are computed online from sea water concentrations (Ziska et al., 2013) using the EMAC submodel AIRSEA (Pozzer et al., 2006) as described by Lennartz et al. (2015). Comprehensive tropospheric and stratospheric chemistry as well as heterogeneous reactions within MECCA (Sander et al., 2011) have been activated for an aerosol surface area concentration climatology.

15 The basic parameter setup has been adopted without changes as proposed by Toyota et al. (2011). The temperature threshold for all simulations has been $T_{\mathrm{crit}} = -15\,°\mathrm{C}$, accordingly.

In EMAC no discrimination is made between FY sea ice and MY sea ice, therefore we initially assume all ice to be first-year (BrXplo_fysic). A multi-year sea ice cover has been computed from RC1SD-base-08 10 hourly SIC output based on ERA-Interim. We regard ice at a fixed location that survived one melting season as multi-year. Hence for simplicity, we assume

20 no drift of ice masses. SIC has been integrated for respective summer months on northern (August/September) and southern (February/March) hemisphere. The SIC at the minimum of the integrated SIC has been chosen as MYSIC for the respective year after. The resulting MYSIC are shown in Fig. 2 together with monthly mean SIC for April (northern hemisphere) and September (southern hemisphere). The result is very similar with regard to patterns and extend of MYSIC on maps retrieved from satellite observation (US National Snow & Ice Data Center (NSIDC), 2017). Based on the MYSIC estimate, a second model integration

25 (BrXplo_mysic) has been conducted. For comparison, a reference simulation with bromine release mechanism switched off has been done (referred to as BrXplo_ref).

3 Results

In this section, we qualitatively compare our simulation results with observational data regarding BrO VCD for both northern and southern hemisphere and depletion events of surface ozone.

30 Since Br_2 released from ice and snow is transformed into BrO photolytically, enhancements of Br_2 result in an increase of BrO vertical column density which is observable by satellite instruments. We use GOME tropospheric VCD of BrO which has been computed from total VCD for solar zenith angles less or equal to $80°$ by subtracting SLIMCAT modeled stratospheric

Table 1. EMAC model experiments used in this study. All experiments have been done using specified dynamics nudged to ERA-Interim. Accordingly, ERA-Interim SIC has been used. The setup is based on the consortial ESCiMo simulation RC1SD-base-08. Experiments have been performed for an assumption of first-year sea ice only (FYSIC) and for a multi-year sea ice cover (MYSIC) estimated from SIC. The temperature threshold for all simulations has been $T_{\mathrm{crit}} = -15\,^\circ\mathrm{C}$, accordingly.

Experiment	Model Version	Resolution	Time-Span	Chemistry	VSLS Emission	Polar Bromine Release
BrXplo_ref	2.52	T42L90MA	Jan–Dec 2000	full	AIRSEA	no
BrXplo_fysic	2.52	T42L90MA	Jan–Dec 2000	full	AIRSEA	FYSIC
BrXplo_mysic	2.52	T42L90MA	Jan–Dec 2000	full	AIRSEA	MYSIC
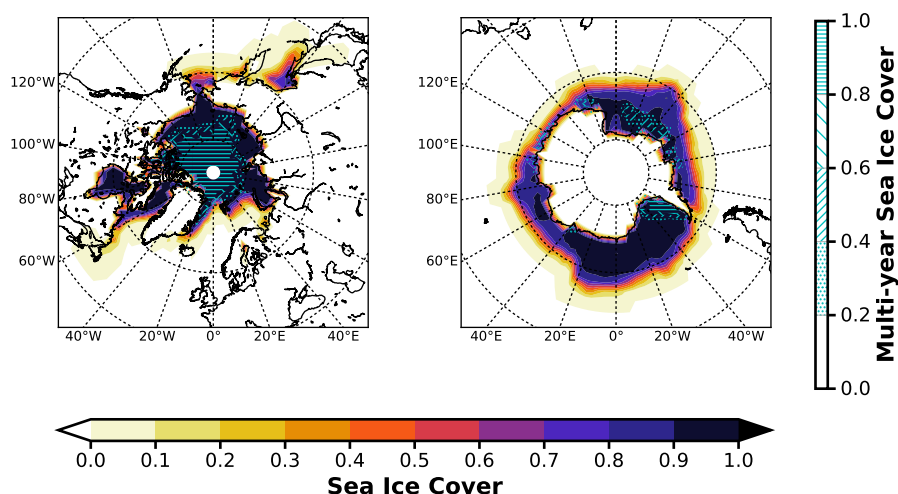
Figure 2. Sea ice cover fraction and estimated multi-year sea ice cover fraction for the year 2000. Mean SIC are shown for April on the northern hemisphere and September on the southern. MYSIC has been computed from RC1SD-base-08 10 hourly SIC based on ERA-Interim. For simplicity, we assume ice that survived one melting season as multi-year. (left) Northern hemisphere; (right) Southern hemisphere.

VCD. Monthly mean tropospheric BrO VCD from GOME-SLIMCAT retrievals are shown in Fig. 3a) for both northern and southern polar regions in April and September, respectively. In April, GOME data display a strong enhancement of BrO VCD across the whole coastal region of the Arctic ocean down to Hudson Bay. There are signs of slight enhancements in the Antarctic coastal regions, where data are available. In September, enhancements above Antarctica are in particular found in the Ross and Weddell sea areas.

From hourly BrO profiles of the EMAC model output, total VCD has been computed and re-sampled in accordance to local solar time 10 UTC, for the ERS-2 equator crossing time had been 10.30 local time. In general, transition times at high latitudes differ from the equator crossing time due to the satellite orbit and total BrO VCD is not directly comparable to tropospheric columns. However, stratospheric columns can be considered constant over space and time (e.g., Richter et al., 1998). Hence, a

qualitative comparison between the two sets of data is sufficiently unaffected by these concerns. The monthly averaged EMAC total BrO VCD are shown in Fig. 3b). Spatial patterns of BrO VCD are reasonably well reproduced by EMAC in Northern hemisphere in April. Compared to GOME, BrO VCD may be underestimated westward from Hudson Bay respectively eastward from the Laptew sea. Regarding the Southern hemisphere in September, BrO VCD is likely overestimated in the model

5 but spatial patterns are rather similar. An overview of monthly mean BrO VCD for both observation and model including all months can be found in Supplement S.3. Apparently, the implemented mechanism is prone for increased BrO VCD shifted to early winter compared to GOME retrievals. A comparison of the BrO VCD spectra of GOME data and simulation implies a good agreement of the first order of magnitude while there are probably missing sources of higher magnitude in the implemented mechanism. But this will be subject to further studies.

10 Regarding depletion events of surface ozone, four different observation sites have been chosen on each hemisphere for comparison (Table 2). However, no data for Arrival Heights and Palmer Station have been available for 2000. Time series of surface ozone VMR are shown in Figures 4–5 including both in situ observations (where available) and model simulations. For each simulation, the nearest grid point has been chosen as representative. In general, we find a good agreement between BrXplo_ref and observations for seasons without bromine release from ice and snow, except for Summit, South Pole station, and Neumayer

15 station in austral winter, where model results are systematically lower compared to observations. In case of BrXplo_fysic all northern hemispheric sites display depletion events in spring as well as in fall. While the depletion events are not entirely in temporal coincidence with observed events, their frequency is generally well reproduced. However, events of ozone depletion in fall are not present in observation data. For Zeppelin Mountain and Alert, these *fault events* are due to the FYSIC assumption. For a decent multi-year sea ice cover is implemented in BrXplo_mysic, they vanish. In case of Barrow, a closer look into

20 spring reveals an astonishing temporal as well as quantitative coincidence of surface ozone VMR especially in April (Fig. 5). The apparent *wiggles* are partly due to hard trigger thresholds T_{crit} and θ_{crit}, but similar structures are in fact apparent in the surface ozone observations at Barrow. Despite the original mechanism's validation for northern hemispheric spring (Toyota et al., 2011), time series for the southern hemisphere do display ozone depletion events in a similar frequency as found in observational data.

4 Discussion and conclusions

Many approaches describing bromine release in the polar regimes rely on modeling of complex micro physical processes which are too detailed for integration in a global chemistry-climate model. We have implemented a bromine release mechanism from sea ice and snow covered land surfaces based on the relatively simple parametrization suggested by Toyota et al. (2011) in the global chemistry-climate model EMAC. While the original study of Toyota et al. (2011) focused on Arctic spring time only, we

30 extend the simulations to the global scale and a full annual cycle. We show that without any further tuning of the parameters, many aspects of observed polar bromine enhancements and boundary layer ozone depletion events are well reproduced by this mechanism within the EMAC model. Resulting spatial patterns of BrO total VCD and the temporal occurrence of surface ozone depletion events are comparable to BrO tropospheric VCD retrieval of the GOME satellite instrument, respectively in situ

Table 2. Observation sites for surface ozone comparison. Providers typeset in italic refer to unavailable data for 2000.

Site	Location	Latitude (°N)	Longitude (°E)	Altitude (m a.s.l.)	Data Provider
Alert	Canada	82.50	-62.30	210	EBAS (NILU)
Barrow	Alaska	71.32	-156.61	8	ESRL/GMD (NOAA)
Zeppelin Mountain	Spitsbergen	78.90	11.88	474	EBAS (NILU)
Summit	Greenland	72.54	-38.48	3238	ESRL/GMD (NOAA)
Palmer Station	Antarctica	-64.77	-64.05	21	*ESRL/GMD (NOAA)*
Neumayer Station	Antarctica	-70.68	-8.26	43	EBAS (NILU)
Arrival Heights	Antarctica	-77.85	166.78	22	*ESRL/GMD (NOAA)*
South Pole Station	Antarctica	-89.98	-24.8	2810	ESRL/GMD (NOAA)

observation at different sites in both the Arctic and Antarctic. EMAC provides a wide range of Earth system related submodels and allows for simulations with full tropospheric and stratospheric (heterogeneous) chemistry in a selfconsistant manner. In our model integrations, inorganic bromine species (HBr, HOBr, BrNO$_3$) are provided in two ways: through photochemical transformation of organic source gases of natural and anthropogenic origin and through descending stratospheric air containing

5   inorganic bromine. The emission of bromine from very short-lived substances (CH$_2$Br$_2$, CHBr$_3$) is consistently computed online from sea water concentrations (Lennartz et al., 2015). However, the implemented bromine release mechanism relies on various assumptions which are not sufficiently well constrained by observations. In particular the dry deposition, which is one of the key factors in this bromine release mechanism, is still highly uncertain and hard to measure explicitly. In a further sensitivity simulation, we have decreased the dry deposition of ozone over snow covered regions as proposed by Helmig et al. (2007) by

10   increasing the surface resistance in DDEP for ozone on snow and ice surfaces from the value of $r_{O_3}^{\text{ice−snow}} = 1/2000\,\text{sm}^{-1}$ (Wesely, 1989) to $r_{O_3}^{\text{ice−snow}} = 1/10000\,\text{sm}^{-1}$ (Helmig et al., 2007). With the reduced dry deposition, ozone depletion events in fall and midwinter are suppressed and the agreement with observed ozone is generally improved (see Supplement S.4). Reducing the ozone dry deposition over snow and ice slightly increases boundary layer ozone at all discussed sites, but even with the reduced dry deposition the model significantly underestimates observed boundary layer ozone in Antarctica, indicating

15   that other mechanisms exist that increase boundary layer ozone under these conditions (e.g., Oltmans, 1981; Helmig et al., 2007).

Although our model simulations with this relatively simple mechanism successfully reproduce many observed features of bromine enhancement and ODEs, there are still notable differences to observations. In particular there is the tendency to generate too high BrO columns and too many ODEs in autumn and mid winter. In addition, some of the parameters like the

20   critical temperature, fixed at $-15\,°\text{C}$, are rather ad hoc and not well constrained by observations. It is possible, that in reality different processes, such as snow-pack chemistry as well as bromine activation by blowing snow, all play a role and contribute

to the bromine explosion events. With the present work we have now a framework to further test these mechanisms in a global chemistry climate model.

Code availability. The Modular Earth Submodel System (MESSy) is continuously further developed and applied by a consortium of institutions. The usage of MESSy and access to the source code is licensed to all affiliates of institutions, which are members of the MESSy

5   Consortium. Institutions can become a member of the MESSy Consortium by signing the MESSy Memorandum of Understanding. More information can be found on the MESSy Consortium Web-site (http://www.messy-interface.org). The modified code of the submodel ONEMIS described here will be made available with the next official release of the MESSy source code distribution.

Data availability. For any party interested, data can be made available on request.

Author contributions. Stefanie Falk has implemented the described mechanism, run and validated the simulations with observational data.

10 Björn-Martin Sinnhuber suggested this study and took part in the analysis. Both authors contributed to the writing of the paper.

Competing interests. The authors declare that they have no conflict of interest.

Acknowledgements. Parts of this work were supported by the Deutsche Forschungsgemeinschaft (DFG) through the research unit 'SHARP' (SI1044/1-2), the German Bundesministerium für Bildung und Forschung (BMBF) through the project 'ROMIC-THREAT' (01GL1217B), and by the Helmholtz Association through its research program 'ATMO'.

15 Ozone in situ data for Alert, Neumayer station, and Zeppelin Mountain have been made available by the Norwegian Institute for Air Research. Database of observation data of atmospheric chemical composition and physical properties, EBAS. http://ebas.nilu.no. Data of Alert are provided by Environment Canada / Atmospheric Environmental Service (EC/AES), data of Neumayer station by Helmholtz-Zentrum Geestacht (HZG), and data of Zeppelin Mountain by Norwegian Institute for Air Research (NILU).

Ozone in situ data for Barrow, Summit, and South Pole station have been provided by U.S. Department of Commerce/National Oceanic &

20 Atmospheric Administration (NOAA) – Earth System Research Laboratory – Global Monitoring Division. https://www.esrl.noaa.gov/gmd/ozwv/surfoz.

Tropospheric BrO column retrievals from GOME instrument have been provided in courtesy of Andreas Richter and John P. Burrows (University of Bremen). The data can be obtained from http://www.iup.uni-bremen.de/doas/gome_bro_data.htm.

We thank Andreas Richter and Astrid Kerkweg for helpful comments on an earlier version of the manuscript.

25 Thanks to Stefan Versick (KIT SimLab Climate and Environment) for technical support concerning the implementation into the EMAC model.
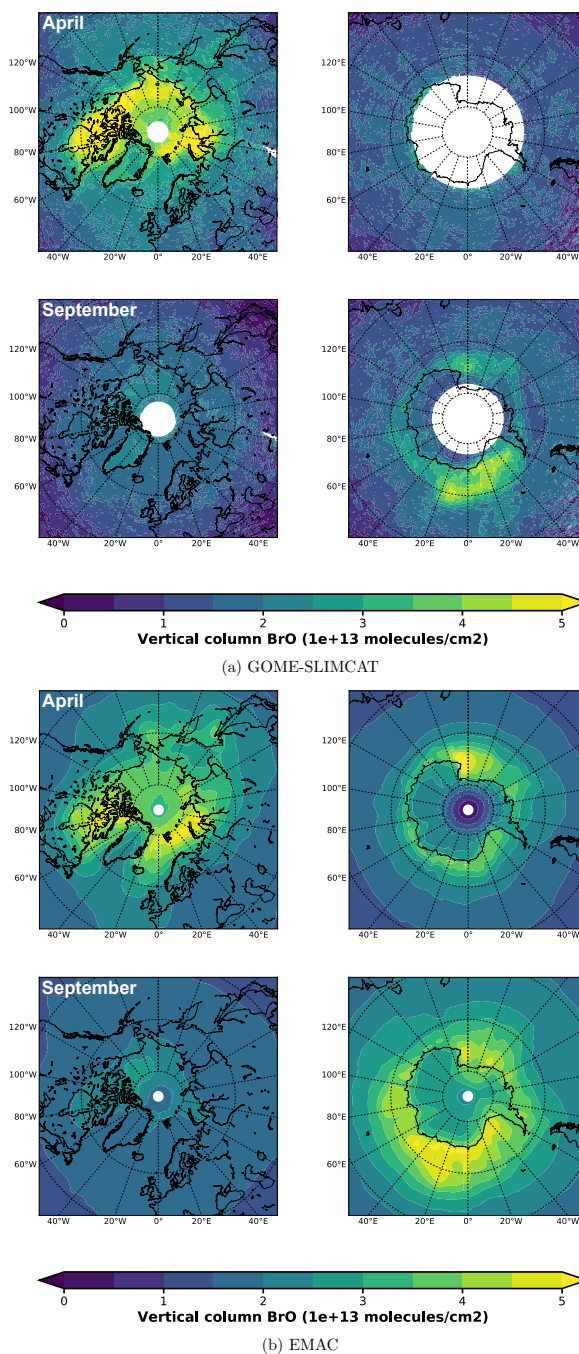
Figure 3. Monthly mean vertical column density of BrO for Arctic and Antarctic spring and austral spring, respectively. EMAC data have been sampled in accordance to local solar time 10 UTC. (a) GOME-SLIMCAT tropospheric; (b) EMAC total.
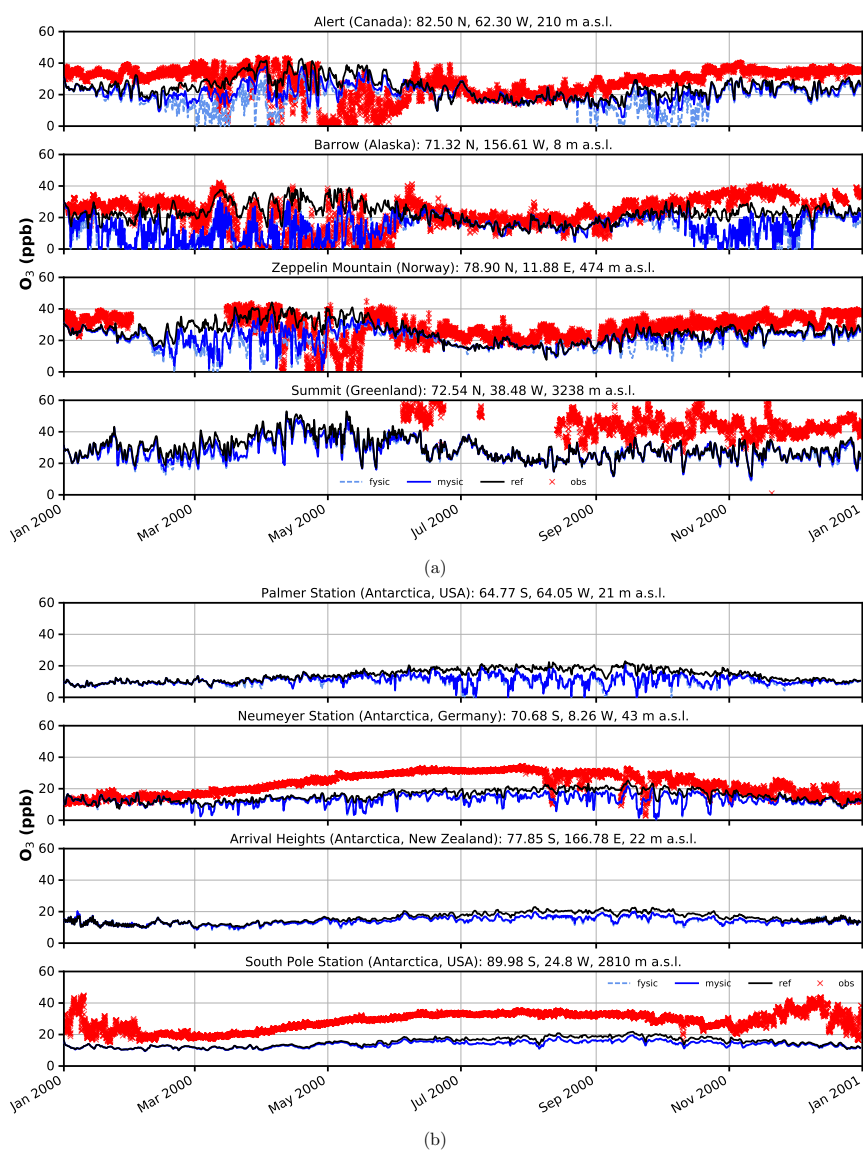
Figure 4. Surface ozone mixing ratios at four different observation sites. Comparison of in situ measurements (red crosses) with results from simulation (solid black – EMAC v2.52 default (no bromine explosions); light blue dashed – FYSIC; solid blue – MYSIC). Representatively, the nearest grid point has been chosen. (a) Northern hemisphere; (b) Southern hemisphere.

(a)

(b)
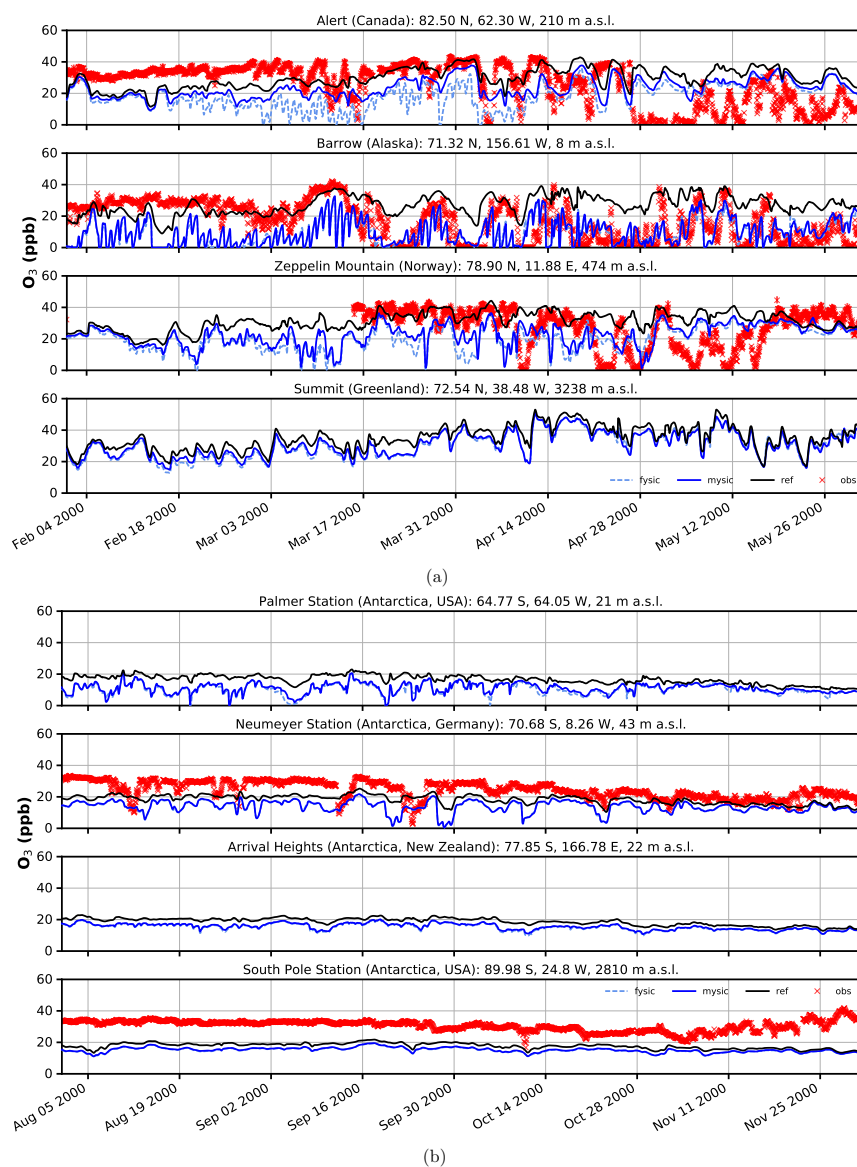
Figure 5. Surface ozone mixing ratios at four different observation sites for spring and austral spring, respectively. Comparison of in situ measurements (red crosses) with results from simulation (solid black – EMAC v2.52 default (no bromine explosions); light blue dashed – FYSIC; solid blue – MYSIC). Representatively, the nearest grid point has been chosen. (a) Northern hemisphere; (b) Southern hemisphere.

References

Bottenheim, J. W., Gallant, A. G., and Brice, K. A.: Measutements of NOy Species and O-3 at 82-Degrees-N Latitude, Geophys. Res. Lett., 13, 113–116, doi:10.1029/GL013i002p00113, 1986.

Bottenheim, J. W., Fuentes, J. D., Tarasick, D. W., and Anlauf, K. G.: Ozone in the Arctic lower troposphere during winter and spring 2000 (ALERT2000), Atmos. Environ., 36, 2535–2544, doi:10.1016/S1352-2310(02)00121-8, 2002.

Bottenheim, J. W., Netcheva, S., Morin, S., and Nghiem, S. V.: Ozone in the boundary layer air over the Arctic Ocean: measurements during the TARA transpolar drift 2006-2008, Atmos. Chem. Phys., 9, 4545–4557, 2009.

Custard, K. D., Thompson, C. R., Pratt, K. A., Shepson, P. B., Liao, J., Huey, L. G., Orlando, J. J., Weinheimer, A. J., Apel, E., Hall, S. R., Flocke, F., Mauldin, L., Hornbrook, R. S., Poehler, D., General, S., Zielcke, J., Simpson, W. R., Platt, U., Fried, A., Weibring, P., Sive, B. C., Ullmann, K., Cantrell, C., Knapp, D. J., and Montzka, D. D.: The NOx dependence of bromine chemistry in the Arctic atmospheric boundary layer, Atmos. Chem. Phys., 15, 10 799–10 809, doi:10.5194/acp-15-10799-2015, 2015.

Helmig, D., Ganzeveld, L., Butler, T., and Oltmans, S. J.: The role of ozone atmosphere-snow gas exchange on polar, boundary-layer tropospheric ozone - a review and sensitivity analysis, Atmos. Chem. Phys., 7, 2007.

Jöckel, P., Kerkweg, A., Pozzer, A., Sander, R., Tost, H., Riede, H., Baumgärtner, A., Gromov, S., and Kern, B.: Development cycle 2 of the Modular Earth Submodel System (MESSy2), Geosci. Model Dev., 3, 717–752, doi:10.5194/gmd-3-717-2010, http://www.geosci-model-dev.net/3/717/2010/, 2010.

Jöckel, P., Tost, H., Pozzer, A., Kunze, M., Kirner, O., Brenninkmeijer, C. A. M., Brinkop, S., Cai, D. S., Dyroff, C., Eckstein, J., Frank, F., Garny, H., Gottschaldt, K.-D., Graf, P., Grewe, V., Kerkweg, A., Kern, B., Matthes, S., Mertens, M., Meul, S., Neumaier, M., Nützel, M., Oberländer-Hayn, S., Ruhnke, R., Runde, T., Sander, R., Scharffe, D., and Zahn, A.: Earth System Chemistry integrated Modelling (ESCiMo) with the Modular Earth Submodel System (MESSy) version 2.51, Geosci. Model Dev., 9, 1153–1200, doi:10.5194/gmd-9-1153-2016, 2016.

Kaleschke, L., Richter, A., Burrows, J., Afe, O., Heygster, G., Notholt, J., Rankin, A. M., Roscoe, H. K., Hollwedel, J., Wagner, T., and Jacobi, H. W.: Frost flowers on sea ice as a source of sea salt and their influence on tropospheric halogen chemistry, Geophys. Res. Lett., 31, doi:10.1029/2004GL020655, 2004.

Kerkweg, A., Buchholz, J., Ganzeveld, L., Pozzer, A., Tost, H., and Jöckel, P.: Technical Note: An implementation of the dry removal processes DRY DEPosition and SEDImentation in the Modular Earth Submodel System (MESSy), Atmos. Chem. Phys., 6, 4617–4632, doi:10.5194/acp-6-4617-2006, http://www.atmos-chem-phys.net/6/4617/2006/, 2006.

Kerkweg, A., Sander, R., Tost, H., and Jöckel, P.: Technical note: Implementation of prescribed (OFFLEM), calculated (ONLEM), and pseudo-emissions (TNUDGE) of chemical species in the Modular Earth Submodel System (MESSy), Atmos. Chem. Phys., 6, 3603–3609, 2006.

Lennartz, S. T., Krysztofiak, G., Marandino, C. A., Sinnhuber, B.-M., Tegtmeier, S., Ziska, F., Hossaini, R., Krüger, K., Montzka, S. A., Atlas, E., Oram, D. E., Keber, T., Bönisch, H., and Quack, B.: Modelling marine emissions and atmospheric distributions of halocarbons and dimethyl sulfide: the influence of prescribed water concentration vs. prescribed emissions, Atmos. Chem. Phys., 15, 11 753–11 772, doi:10.5194/acp-15-11753-2015, http://www.atmos-chem-phys.net/15/11753/2015/, 2015.

Lindberg, S. E., Brooks, S., Lin, C. J., Scott, K. J., Landis, M. S., Stevens, R. K., Goodsite, M., and Richter, A.: Dynamic oxidation of gaseous mercury in the Arctic troposphere at polar sunrise, Envir. Sci. Tech., 36, 1245–1256, doi:10.1021/es0111941, 2002.

Oltmans, S. J.: Surface Ozone Measurements In Clean-Air, J. Geophys. Res.-Oceans Atmos., 86, 1174–1180, doi:10.1029/JC086iC02p01174, 1981.

Pozzer, A., Jöckel, P. J., Sander, R., Williams, J., Ganzeveld, L., and Lelieveld, J.: Technical note: the MESSy-submodel AIRSEA calculating the air-sea exchange of chemical species, Atmos. Chem. Phys., 6, 5435–5444, 2006.

5 Pratt, K. A., Custard, K. D., Shepson, P. B., Douglas, T. A., Pöhler, D., General, S., Zielcke, J., Simpson, W. R., Platt, U., Tanner, D. J., Huey, L. G., Carlsen, M., and Stirm, B. H.: Photochemical production of molecular bromine in Arctic surface snowpacks, Nat. Geosci., 6, 351–356, doi:10.1038/NGEO1779, 2013.

Richter, A., Wittrock, F., Eisinger, M., and Burrows, J. P.: GOME observations of tropospheric BrO in northern hemispheric spring and summer 1997, Geophys. Res. Lett., 25, 2683–2686, doi:10.1029/98GL52016, 1998.

10 Richter, A., Wittrock, F., Ladstatter-Weissenmayer, A., and Burrows, J. P.: GOME measurements of stratospheric and tropospheric BrO, in: REMOTE SENSING OF TRACE CONSTITUENTS IN THE LOWER STRATOSPHERE, TROPOSPHERE AND THE EARTH'S SURFACE: GLOBAL OBSERVATIONS, AIR POLLUTION AND THE ATMOSPHERIC CORRECTION, edited by Burrows, J. P. and Takeucki, N., vol. 29 of *Adv. Space. Res.*, pp. 1667–1672, Comm Space Res, doi:10.1016/S0273-1177(02)00123-0, A1 2 Symposium of COSPAR Scientific Commission A held at the 33rd COSPAR Scientific Assembly, WARSAW, POLAND, JUL, 2000, 2002.

15 Roeckner, E., Brokopf, R., Esch, M., Giorgetta, M., Hagemann, S., Kornblueh, L., Manzini, E., Schlese, U., and Schulzweida, U.: Sensitivity of simulated climate to horizontal and vertical resolution in the ECHAM5 atmosphere model, J. Climate, 19, 3771–3791, doi:10.1175/JCLI3824.1, 2006.

Saiz-Lopez, A. and von Glasow, R.: Reactive halogen chemistry in the troposphere, Chem. Soc. Rev., 41, 6448–6472, doi:10.1039/c2cs35208g, 2012.

20 Sander, R., Baumgaertner, A., Gromov, S., Harder, H., Jöckel, P., Kerkweg, A., Kubistin, D., Regelin, E., Riede, H., Sandu, A., Taraborrelli, D., Tost, H., and Xie, Z.-Q.: The atmospheric chemistry box model CAABA/MECCA-3.0, Geosci. Model Dev., 4, 373–380, doi:10.5194/gmd-4-373-2011, http://www.geosci-model-dev.net/4/373/2011/, 2011.

Sander, R., Burrows, J., and Kaleschke, L.: Carbonate precipitation in brine - a potential trigger for tropospheric ozone depletion events, Atmos. Chem. Phys., 6, 4653–4658, 2006.

25 Simpson, W. R., von Glasow, R., Riedel, K., Anderson, P., Ariya, P., Bottenheim, J., Burrows, J., Carpenter, L. J., Friess, U., Goodsite, M. E., Heard, D., Hutterli, M., Jacobi, H.-W., Kaleschke, L., Neff, B., Plane, J., Platt, U., Richter, A., Roscoe, H., Sander, R., Shepson, P., Sodeau, J., Steffen, A., Wagner, T., and Wolff, E.: Halogens and their role in polar boundary-layer ozone depletion, Atmos. Chem. Phys., 7, 4375–4418, 2007.

Stephens, C. R., Shepson, P. B., Steffen, A., Bottenheim, J. W., Liao, J., Huey, L. G., Apel, E., Weinheimer, A., Hall, S. R., Cantrell, C., Sive,

30 B. C., Knapp, D. J., Montzka, D. D., and Hornbrook, R. S.: The relative importance of chlorine and bromine radicals in the oxidation of atmospheric mercury at Barrow, Alaska, J. Geophys. Res.-Atmos., 117, doi:10.1029/2011JD016649, 2012.

Toyota, K., McConnell, J. C., Lupu, A., Neary, L., McLinden, C. A., Richter, A., Kwok, R., Semeniuk, K., Kaminski, J. W., Gong, S. L., Jarosz, J., Chipperfield, M. P., and Sioris, C. E.: Analysis of reactive bromine production and ozone depletion in the Arctic boundary layer using 3-D simulations with GEM-AQ: inference from synoptic-scale patterns, Atmos. Chem. Phys., 11, 3949–3979, doi:10.5194/acp-11-

35 3949-2011, 2011.

US National Snow & Ice Data Center (NSIDC): EASE-Grid Sea Ice Age, online, http://nsidc.org/soac/sea-ice-age-year.html#seaiceagesequential, 2017.

Wesely, M. L.: Parameterization Of Surface Resistances To Gaseous Dry Deposition In Regional-Scale Numerical-Models, Atmos. Environ., 23, 1293–1304, doi:10.1016/0004-6981(89)90153-4, 1989.

Yang, X., Pyle, J. A., Cox, R. A., Theys, N., and Van Roozendael, M.: Snow-sourced bromine and its implications for polar tropospheric ozone, Atmos. Chem. Phys., 10, 7763–7773, doi:10.5194/acp-10-7763-2010, 2010.

5 Ziska, F., Quack, B., Abrahamsson, K., Archer, S. D., Atlas, E., Bell, T., Butler, J. H., Carpenter, L. J., Jones, C. E., Harris, N. R. P., Hepach, H., Heumann, K. G., Hughes, C., Kuss, J., Krüger, K., Liss, P., Moore, R. M., Orlikowska, A., Raimund, S., Reeves, C. E., Reifenhäuser, W., Robinson, A. D., Schall, C., Tanhua, T., Tegtmeier, S., Turner, S., Wang, L., Wallace, D., Williams, J., Yamamoto, H., Yvon-Lewis, S., and Yokouchi, Y.: Global sea-to-air flux climatology for bromoform, dibromomethane and methyl iodide, Atmos. Chem. Phys., 13, 8915–8934, doi:10.5194/acp-13-8915-2013, 2013.